

Supplemental information

BCAT1 redox function maintains mitotic fidelity

Liliana Francois, Pavle Boskovic, Julian Knerr, Wei He, Gianluca Sigismondo, Carsten Schwan, Tushar H. More, Magdalena Schlotter, Jeroen Krijgsveld, Karsten Hiller, Robert Grosse, Peter Lichter, and Bernhard Radlwimmer

Figure S1. BCAT1 localizes to the nucleus and mitotic structures in tumor cells *in vitro* and *in vivo*.

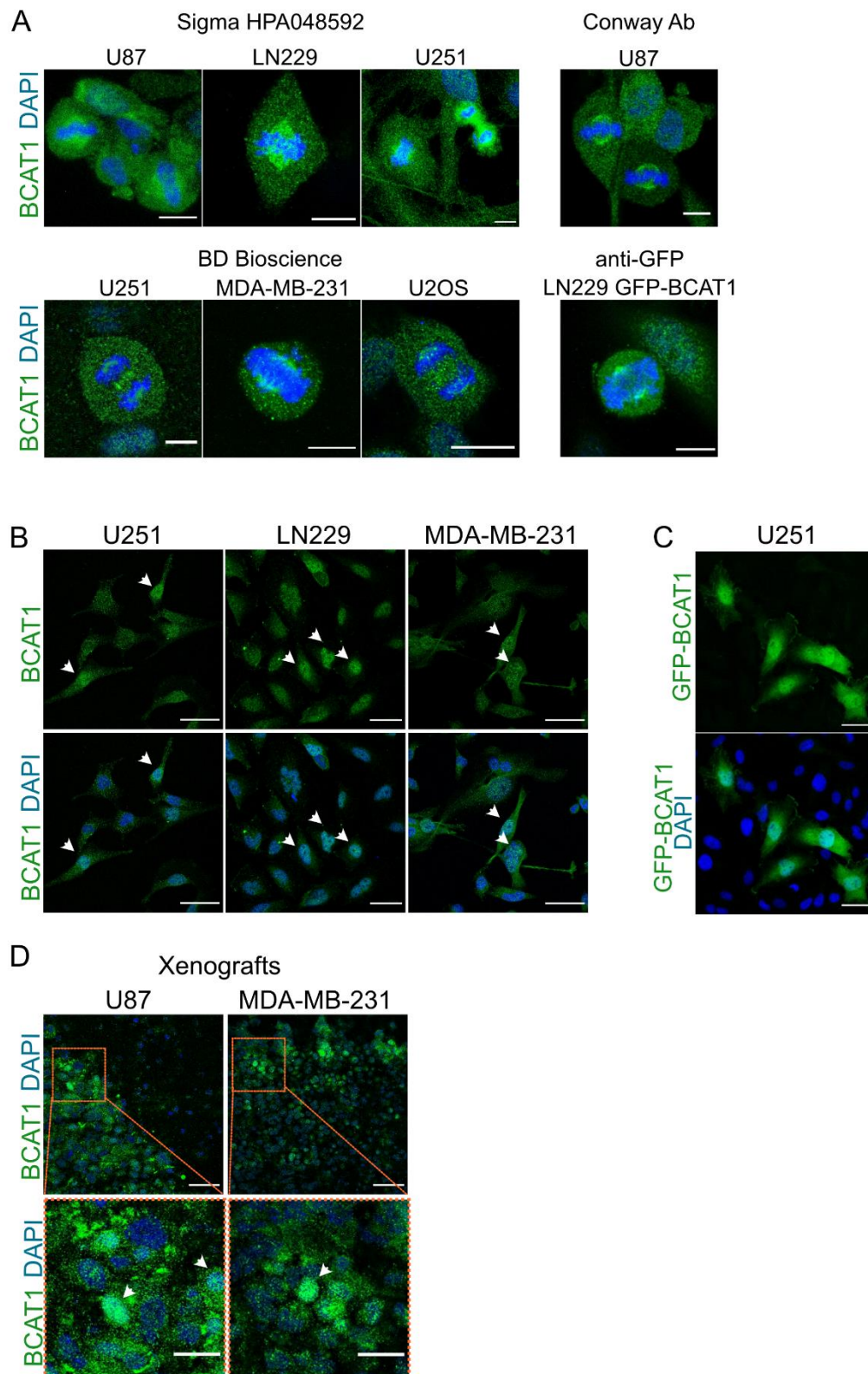


Figure S1. BCAT1 localizes to the nucleus and mitotic structures in tumor cells *in vitro* and *in vivo*.

(A) Localization of BCAT1 at the spindle of multiple cancer cell lines was confirmed using different antibodies against BCAT1.

Sigma HPA048592, rabbit polyclonal Ab, 1:100

Antibody kindly provided by Prof. Dr. Myra Conway (Bristol, UWE), rabbit polyclonal, 1:200

BD Biosciences ECA39/Clone 51, mouse monoclonal, 1:100

Anti-GFP, rabbit 1:200, used in cell expressing GFP-BCAT1.

(B-D) BCAT1 distributes throughout the cytoplasm and localizes in the nucleus (arrowheads) of tumor cells *in vitro* (B) and *in vivo* (C).

(B) BCAT1 immunofluorescence in glioblastoma (U251 and LN229) and breast carcinoma (MDA-MB-231) cells *in vitro*. Scale bar = 50 μ m

(C) Example images of GFP-BCAT1 localizing at the nucleus and cytoplasm of U251 cells transiently transfected GFP-BCAT1.

(D) Histological sections of cell line-derived mouse xenografts. Arrows point to BCAT1 signal in the nucleus of glioblastoma (U87) and breast carcinoma (MDA-MB-231) cells. Scale bar = 50 μ m, insets scale bar = 20 μ m

Related to Figure 1

Figure S2. Characterization of BCAT1 knockout cell lines

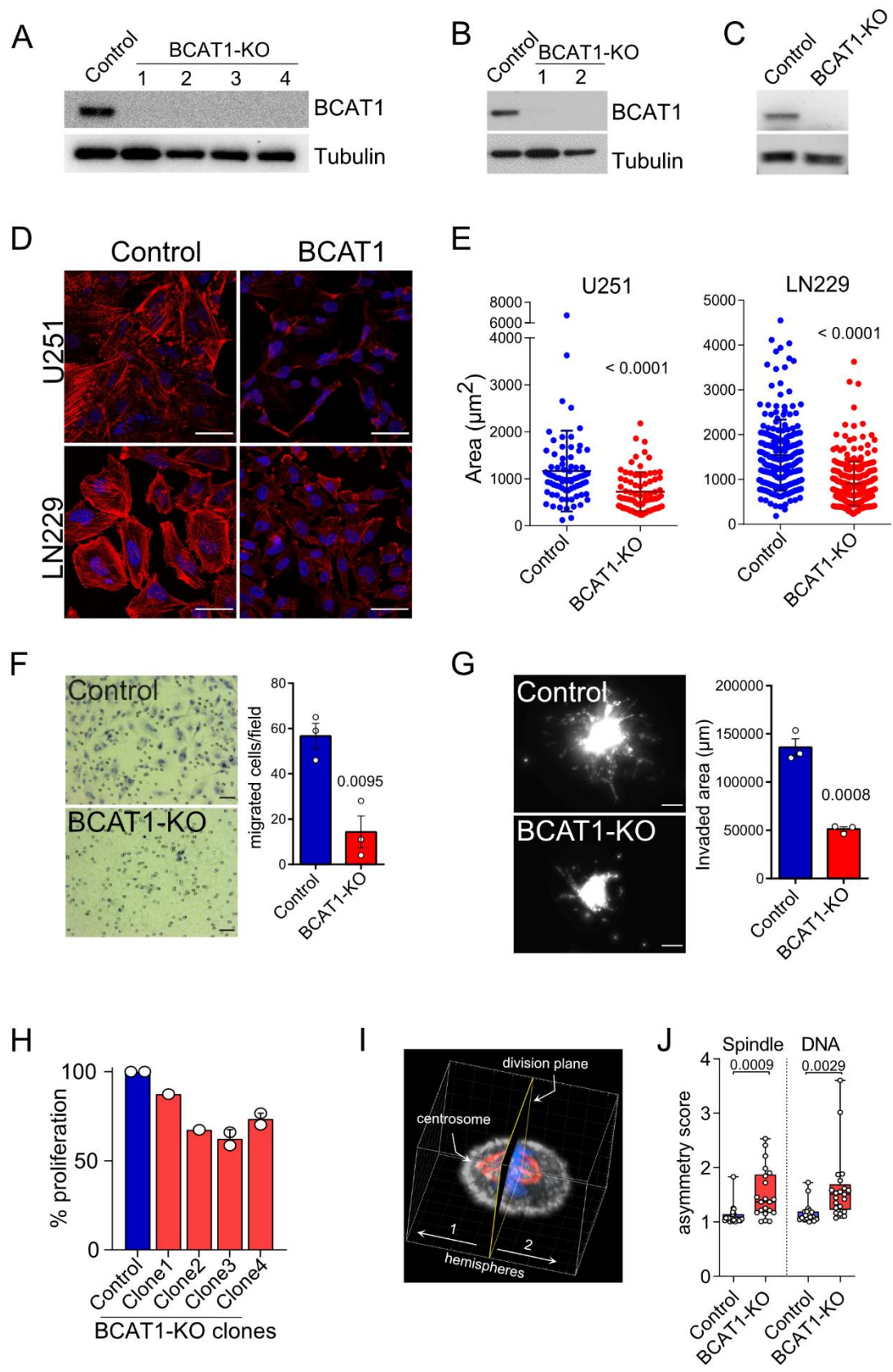


Figure S2. Characterization of BCAT1 knockout cell lines

(A-C) Western blot confirming efficient CRISPR-mediated knockout of BCAT1 (BCAT1-KO) in multiple single cell clones of U251 (A), LN229 (B) and MDA-MB-231 (C).

(D-E) Morphological changes observed in BCAT1 Knockout (BCAT1-KO) cells. Representative pictures (D) and quantification of cell area (E) in LN229 and U251. Cell area was calculated using Fiji (ImageJ) after segmentation of individual cells using F-actin signal (red). N > 210 cells were quantified per condition, 2 biological replicates. Scale bar = 50 μ m. Unpaired, two-sided t-test.

(F) Migration of U251 cells assessed by transwell migration assay. Scale bar = 50 μ m. N = 3 biological replicates. Data points correspond to the mean number of migrated cells counted in 5 fields of view per experiment. Bars = mean of migrated cells of 3 experiments \pm s.e.m. Unpaired, two-sided t-test.

(G) Ex vivo organotypic invasion assay. LN229 control or BCAT1-KO were grown as spheroids and implanted into the cortex of freshly cut mouse brains. Invaded area was quantified 2 days after implantation. Representative images of 3 independent experiments, at least 10 implanted spheroids per experiments were quantified. Scale bar on images = 100 μ m. White dots = mean invaded area of 10 spheroids per experiment. Bars = mean invaded area of the 3 experiments \pm s.e.m. Unpaired, two-sided t-test.

(H) EdU incorporation Click-iT assay showing reduced cell proliferation in U251 BCAT1-KO clones.

(I-J) symmetry ratio of spindle and DNA alignment obtained from mitotic spindles of LN229 control and BCAT1-KO cells. (I) depicts how the division plane was defined: 3D renderings were separated orthogonally to the line connecting the centrosomes (determined by Centrin-1 staining). The volume of spindle (Tubulin, red) and DNA (DAPI, blue) of each hemisphere is obtained and the value of one side is divided by the value other side (symmetry score = Vol1/Vol2). To obtain positive values, the larger value was divided by the smaller one. Control, N 20; BCAT1-KO, N=21. Unpaired, two-sided t-test.

Related to Figure 1 and Video S2.

Figure S3. BCAT1-KO cause G2/M arrest in cancer and iPS cells

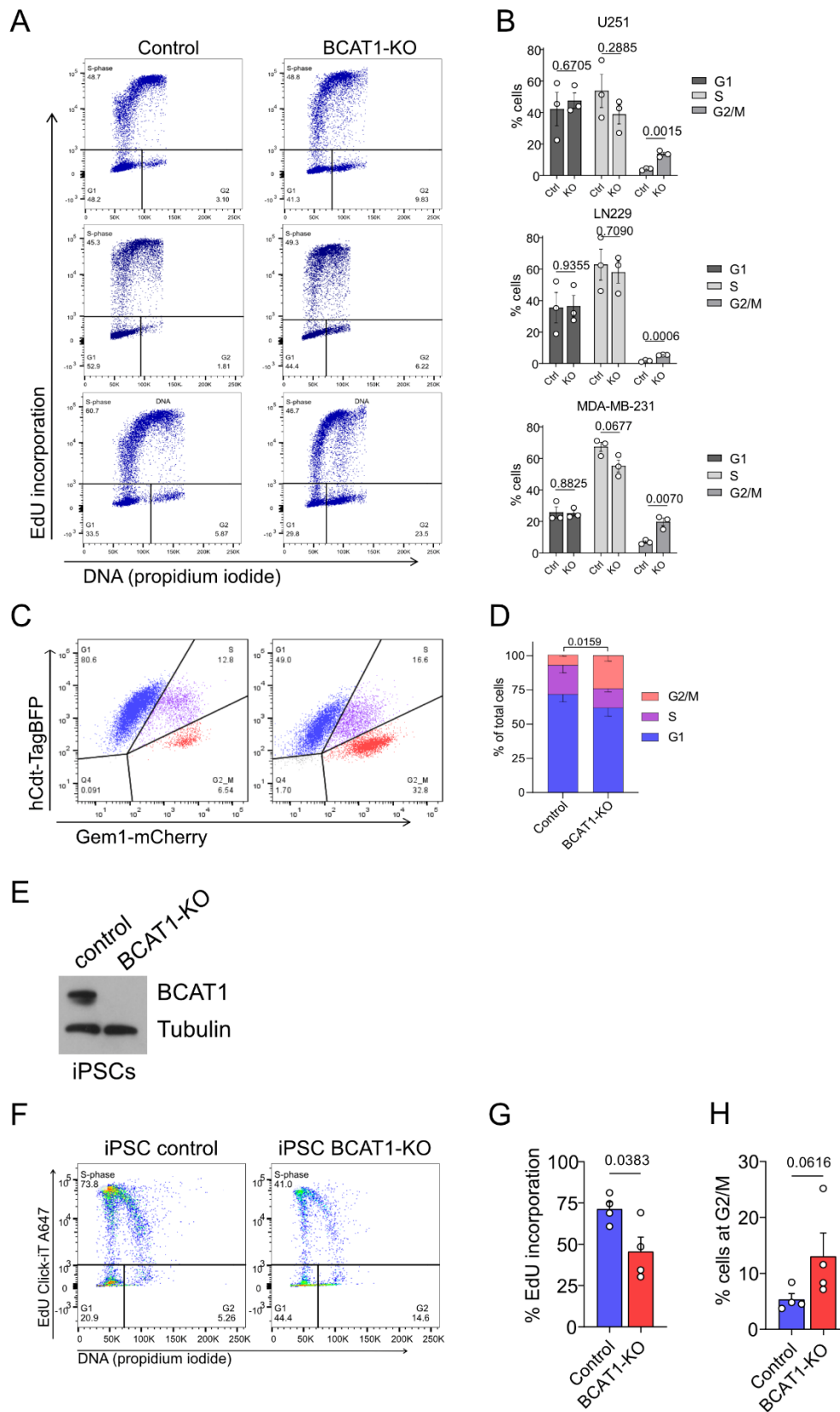


Figure S3. BCAT1-KO cause G2/M arrest in cancer and iPS cells

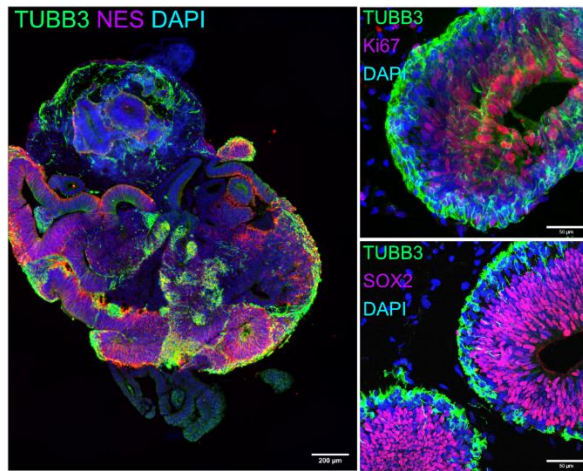
- (A) Representative dot plots and
- (B) Quantification of flow cytometry analysis of the cell cycle using Click-iT™ EdU incorporation and DNA staining. Quantification of percentage of at each cell cycle phase in three different cancer cell lines. Bars are mean values \pm s.e.m of 3 independent experiments. Unpaired, two-sided t-test.
- (C) Representative dot plots and
- (D) quantification of flow cytometry analysis of the cell cycle distribution in U251 cells expressing the FUCCI cell cycle system. Bars are mean values \pm s.e.m of 3 independent experiments. Unpaired, two-sided t-test.
- (E) Western blot confirming efficient CRISPR-mediated knockout of BCAT1 (BCAT1-KO) iPSCs.
- (F) iPSCs were pulsed with EdU for 2-4hr, then fixed and subjected to Click-iT (Invitrogen). For analysis of DNA content, samples were stained with propidium iodide (PI) 30 minutes before imaging. Representative dot plots of flow cytometry analysis of cell cycle distribution. EdU positive cells marked proliferating cell population.
- (G) Quantification of percentage of EdU positive cells.
- (H) Percentage of cells at G2/M phase in 4 independent experiments.

In G and H, bars are mean values \pm s.e.m of at least 4 biological replicates. Unpaired, two-sided student's t-test.

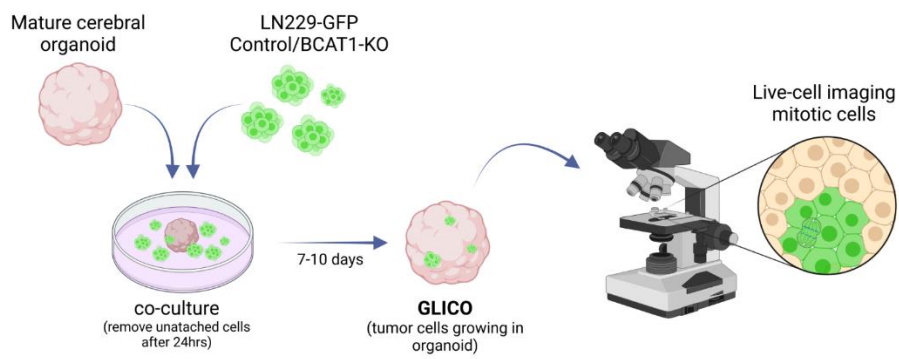
Related to Figure 2 and Video S3.

Figure S4. BCAT1-KO impacts growth and mitosis in GLICO

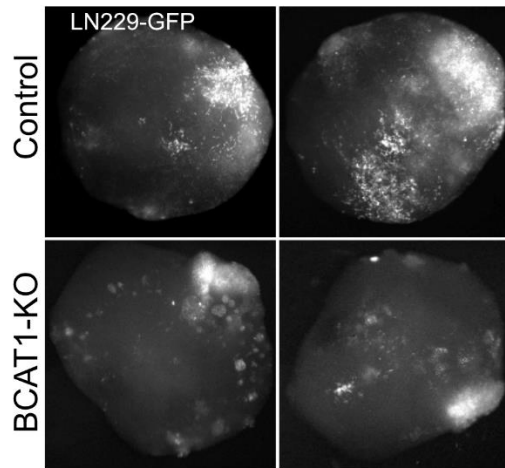
A



B



C



D

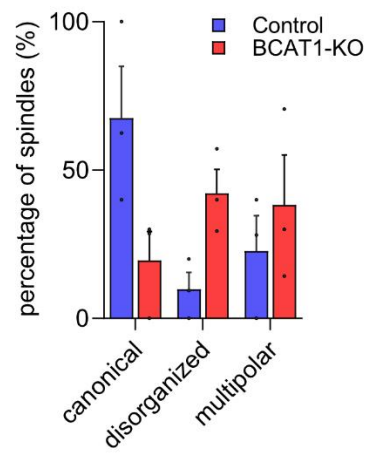


Figure S4. BCAT1-KO impacts growth and mitosis in GLICO

- (A) Representative immunofluorescence images of mature human cerebral organoids (DIV>25). To confirm organization and maturity of organoids, histological sections were stained against the neuronal marker TUBB3, neural stem/progenitor marker Nestin (NES). SOX2 and Ki67 show active proliferation of stem cells in neural rosettes
- (B) Schematic of the procedure for GLICO. GFP-expressing LN229 control and BCAT1 KO spheroid cultures were co-cultured with mature cerebral organoids for 24 hrs and then allowed to grow for 10-14 days until live-cell imaging.
- (C) Representative stereotaxic images of organoids bearing LN229-GFP Control or BCAT1-KO cells demonstrating efficient implantation and tumor formation within the organoids. Left and right images are opposite sides of the same organoid, showing different growth patterns between control and BCAT1-KO cells.
- (D) Frequency of canonical and non-canonical spindle observed in control and BCAT1-KO LN229 cells imaged in the GLICO model. Bars are mean values \pm s.e.m. At least 10 cells were imaged per organoid. N=3 organoids per condition).

Related to Figure 3A-3D and Video S5

Figure S5. BCAT1-KO affects AURKB and TTK activity

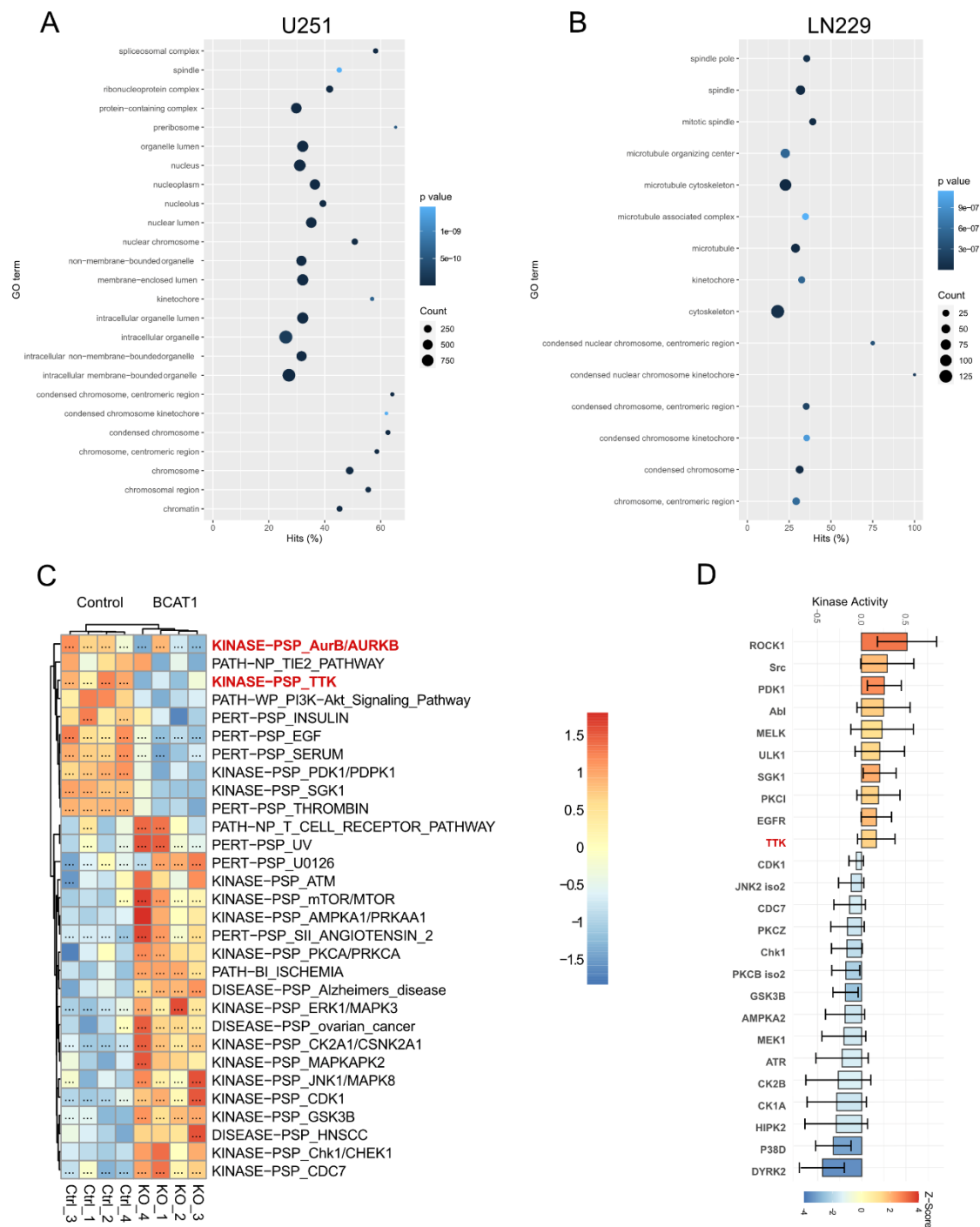


Figure S5. BCAT1-KO affects AURKB and TTK activity

- (A-B) GO Enrichment analysis of genes differentially expressed between mitotic and unsynchronized U251 (A) and LN229 (B) cells using whole proteome data. The analysis was performed using genes with adjusted p values of <0.01 , dot color represents the p-value of a GO term enrichment and the size corresponds to the number of features.
- (C) Phosphosite-specific ssGSEA analysis was performed on the 4 control and BCAT1-KO mitotic U251 phosphoproteomics samples against the PTMsigDB dataset, the same as described in Figure 4. The 30 signatures with the highest median difference between the two groups are presented in the normalized enrichment score (NES) heatmap transformed as z-scores (color scale). Significantly enriched signatures (adjusted p value <0.01) in each sample are denoted by “...”
- (D) Kinase substrate enrichment analysis performed on differentially phosphorylated phosphosites between mitotic U251 control and BCAT1-KO cells using the RoKAI App, as described in Figure 4.

Related to Figure 4.

Figure S6. BCAT1 affects AURKB localization and function

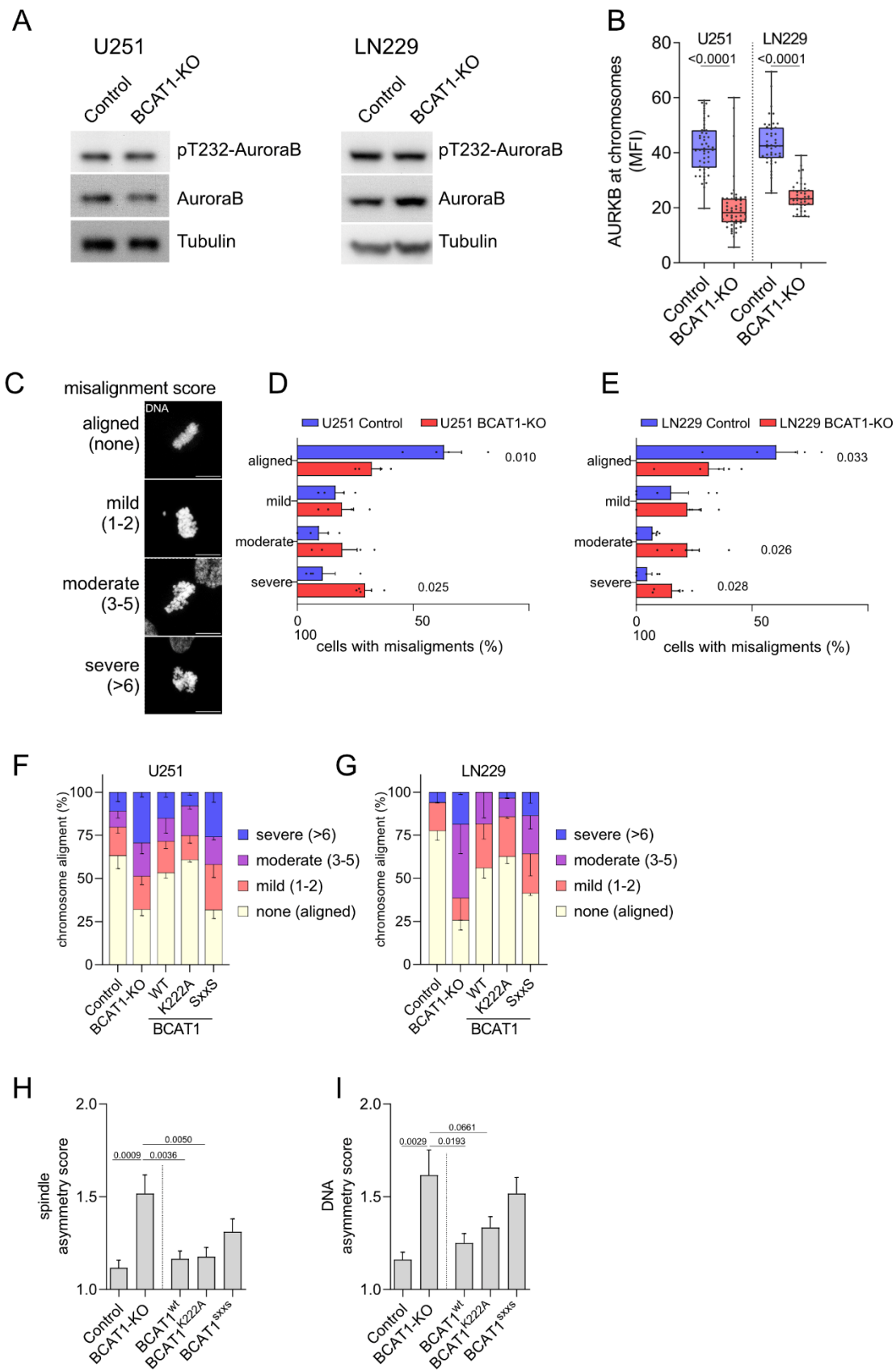


Figure S6. BCAT1 affects AURKB localization and function

(A) Immunoblots against phospho-T232 Aurora B showing similar expression of pT232 and total AURKB in U251 and LN229 mitotic cells.

(B) Localization of AURKB at the chromosome in cells arrested in metaphase. AURKB signal at the centromere was quantified at the area defined by DAPI signal. Mean (horizontal lines) \pm s.d. (vertical lines); U251 Control (n=52), U251 BCAT1-KO (n=50); LN229 Control (n=43), LN229 BCAT1-KO (n=43); total number of cells were acquired from at least 3 biological replicates; P values calculated using unpaired two-sided student t-test.

(C) Examples pictures of chromosomal alignment in cells arrested in metaphase. Cells were treated as described in (B). Alignment score was determined by the number of observed chromosomes deviating from the metaphase plane: none (all chromosomes aligned), mild (1-2 chromosomes), moderate (3-5 chromosomes), severe (>6 chromosomes or failed alignment).

(D-E) quantification of chromosome misalignments in U251 (D) and LN229 (E). Categorization was done as described in (C). Bars are mean values \pm s.e.m of 4 biological replicates. Unpaired, two-sided student's t-test.

(F-G) rescue of chromosome alignment in U251 (E) and LN229 (F) Control, BCAT1-KO and BCAT1-KO expressing the indicated BCAT1 mutants. Cells were treated and analyzed as described in (C). U251 Control (n=95), U251 BCAT1-KO (n=89), U251-BCAT1^{WT} (n=40), U251-BCAT1^{K222A} (n=42), U251-BCAT1^{SxxS} (n=43); LN229 Control (n=43), LN229 BCAT1-KO (n=43); LN229-BCAT1^{WT} (n=29), LN229-BCAT1^{K222A} (n=29), LN229-BCAT1^{SxxS} (n=14). For U251, N=3 biological replicates; LN229, N=2 biological replicates.

(H-I) rescue of symmetry positioning of the spindle and DNA. Scores were calculated as described in Figure S2I. LN229 Control (n=20), LN229 BCAT1-KO (n=21); LN229-BCAT1^{WT} (n=19), U251-BCAT1^{K222A} (n=20), U251-BCAT1^{SxxS} (n=25). N=2 biological replicates.

Related to Figure 6.